Pyrite-mediated advanced oxidation processes: applications, mechanisms, and enhancing strategies

Biao Song[a,b,c], Zhuotong Zeng[b], Eydhah Almatrafi[c], Maocai Shen[a], Weiping Xiong[a,b,c], Chengyun Zhou[a,b,c], Wenjun Wang[a], Guangming Zeng[a,b,c,*], Jilai Gong[a,b,c,*]

[a] College of Environmental Science and Engineering and Key Laboratory of Environmental Biology and Pollution Control (Ministry of Education), Hunan University, Changsha 410082, PR China

[b] Department of Dermatology, Second Xiangya Hospital, Central South University, Changsha 410011, PR China

[c] Center of Research Excellence in Renewable Energy and Power Systems, Center of Excellence in Desalination Technology, Department of Mechanical Engineering, Faculty of Engineering-Rabigh, King Abdulaziz University, Jeddah 21589, Saudi Arabia

* Corresponding authors at College of Environmental Science and Engineering, Hunan University, Changsha 410082, PR China.

Tel: +86 731 88822754; Fax: +86 731 88823701.

E-mail addresses: zgming@hnu.edu.cn (G. Zeng); jilaigong@hnu.edu.cn (J. Gong)

Abstract

Proper treatment of wastewater is one of the key issues to the sustainable development of human society, and people have been searching for high-efficiency and low-cost methods for wastewater treatment. This article reviews recent studies about pyrite-mediated advanced oxidation processes (AOPs) in removing refractory organics from wastewater. The basic information of pyrite and its characteristics for AOPs are first introduced. Then, the performance and mechanisms of pyrite-mediated Fenton oxidation, electro-Fenton oxidation, and persulfate oxidation processes are carefully reviewed and presented. Natural pyrite is an abundant low-cost heterogeneous catalyst for AOPs, and the slow release of Fe^{2+} and the self-regulation of solution pH are highlighted characteristics of pyrite-mediated AOPs. In AOPs, the interaction between Fe^{3+} and pyrite facilitates the Fe^{2+} regeneration and the Fe^{2+}/Fe^{3+} cycle. Making pyrite into nanoparticles, assisting by ultrasound and light irradiation, and adding exogenous Fe^{3+}, organic chelating agents, or biochar is effective to enhance the performance of pyrite-mediated AOPs. Based on the analyses of those pyrite-mediated AOPs and their enhancing strategies, the future development directions are proposed in the aspects of toxicity research, mechanism research, and technological coupling.

Keywords: Pyrite; Advanced oxidation process; Organic wastewater; Water treatment

1. Introduction

Wastewater treatment is essential to pollutant discharge reduction and water-use efficiency improvement. The rapid development of petroleum, chemical engineering, textiles, dyeing, food, pharmacy, metallurgy and other industries in modern society has caused large production of organic wastewater, which often contains refractory and highly toxic organics such as polycyclic aromatic hydrocarbons, halogenated hydrocarbons, phthalic acid esters, pharmaceuticals, and insecticides (Cai et al. 2021). If untreated the organic wastewater may cause severe damage to ecological environment and human health (Gwenzi and Chaukura 2018). However, conventional biological methods adopted by municipal sewage treatment plants are insufficient to completely eliminate refractory organics from industrial wastewater, especially those with limited bioavailability (Grandclément et al. 2017). Considering the increasingly serious environmental pollution and water resource shortage today, exploring innovative technologies for organic wastewater treatment and recycling is urgently needed.

Advanced oxidation processes (AOPs) are typical effective methods to manage high-concentration refractory organics in wastewater. AOPs utilize electricity, light irradiation, ultrasound or catalysts to activate oxidants for producing active free radicals with extremely oxidizing capacity, and then realize the degradation even direct mineralization of organic compounds via the attack of the free radicals (Ma et al. 2021). For instance, the hydroxyl radical (·OH) generated in AOPs possesses a high oxidation potential of 2.80 V, and the oxidizing capacity of ·OH far exceeds those of common

chemical oxidants (e.g., permanganate, H_2O_2, and O_3), sufficient to degrade most organic pollutants non-selectively (Boczkaj and Fernandes 2017). Common AOPs include chemical catalytic oxidation, electrochemical catalytic oxidation, ozonation, and photocatalytic oxidation. Transforming toxic organics into CO_2 and H_2O by AOPs is environmentally friendly, but the high costs of conventional AOPs (involving power, chemicals, and sludge management) limit their large-scale practical applications (Mousset et al. 2021). Additionally, it is difficult to control the optimal proportion of catalyst/oxidant and maintain the solution pH during conventional AOPs (Zhang et al. 2019a). Thus, the researchers have been working on seeking high efficiency and low-cost catalytic materials for AOPs.

Pyrite is a plentiful sulfide mineral found in nature, and it is the main raw material for producing sulfur and sulfuric acid (Oliveira et al. 2012). In the past decades, the geochemical characteristics, mineral dressing, and acid mine drainage of pyrite have been widely studied. Besides, pyrite shows great potential in solving some environmental problems, such as stabilization of hexavalent chromium (Li et al. 2020c), chemical adsorption of arsenic (Bulut et al. 2014), abiotic dechlorination of chlorinated organics (Demiya et al. 2018), hydrolytic removal of microcystins (Fang et al. 2020), and denitrification removal of nitrate (Si et al. 2021). In the aspect of AOPs, pyrite is an attractive catalyst. The oxidation of pyrite in aqueous solution generates many intermediate products such as Fe^{2+}, S^0, H_2S, and polysulfides, which are active in advanced oxidation reactions (Feng et al. 2019). In recent years, many successful experimental studies about pyrite catalyst for AOPs have been reported, especially for

Fenton oxidation and persulfate oxidation, and the research enthusiasm continues. However, to our knowledge, currently there is a lack of timely review on this topic to provide the basic understanding and guide the further research. In this article, recent studies about pyrite-mediated AOPs are carefully reviewed. The basic information of pyrite and its characteristics for AOPs are first introduced. Primary focus is placed on the performance and mechanisms of pyrite-mediated Fenton oxidation, electro-Fenton oxidation, and persulfate oxidation processes. Some enhancing strategies and future research needs for pyrite-mediated AOPs are presented. This review article is hoped to give basic information and reference on pyrite-mediated AOPs and advance their further research and practical applications.

2. Pyrite and its characteristics for AOPs

Pyrite is a sulfide mineral, which is widespread in hydrothermal veins, polymetallic ore deposits, metamorphic rocks, and igneous rocks (Migaszewski and Gałuszka 2019). The main composition of pyrite is disulphide of iron (FeS_2), and it presents with a face-centered cubic lattice in the crystal structure. In natural pyrite, partial substitution of iron by other metal elements (e.g., nickel, cobalt, and copper) may occur (Abraitis et al. 2004). Due to the characteristics of light brassy color and metallic luster, pyrite is often mistaken for gold and thus also known as "Fool's Gold" (Gregory and Kohn 2020). Oxidation and dissolution characteristics of pyrite in aqueous solutions are research hotspot in the field of geochemistry and environment. The dissolved Fe^{2+} from pyrite can serve as catalyst in AOPs to achieve effective

degradation of refractory organic pollutants. Oxygen and Fe^{3+} are two important oxidizers for pyrite oxidation in aqueous solutions, and the oxidation processes can be expressed as Eqs. (1) and (2). Significantly, Fe^{3+} was reported to be more aggressive and powerful than O_2 for pyrite oxidation, and oxidation rates by Fe^{3+} were nearly one and two orders of magnitude higher than that by O_2 at high and low pH, respectively (Chandra and Gerson 2010). Therefore, taking full advantage of the oxidation characteristics of pyrite to offer Fe^{2+} for AOPs has become a hot topic.

$$2FeS_2 + 7O_2 + 2H_2O \rightarrow 2Fe^{2+} + 4SO_4^{2-} + 4H^+ \quad (1)$$

$$FeS_2 + 14Fe^{3+} + 8H_2O \rightarrow 15Fe^{2+} + 2SO_4^{2-} + 16H^+ \quad (2)$$

For catalytic applications in AOPs, natural pyrite has excellent machinability. Many researchers used natural pyrite materials obtained from local mines, mining companies, and chemical reagent companies in their study of AOPs. Before being used as a catalyst for AOPs, pyrite usually undergoes a pretreatment of grinding, sieving, removing impurities, washing, and drying (He et al. 2021). The typical processing steps are illustrated in Fig. 1a. In a typical pretreatment process, pyrite ore is ground into fine powders by a ceramic or agate mortar, and then sieved to smaller particles at a micron level. Subsequently, the oxide impurities on pyrite surface are removed by acid pickling. After being washed by deoxygenated deionized water, the pyrite catalyst is dried in an oxygen-free oven. Through simple processing and preparation, high-performance pyrite catalyst can be obtained from the natural mineral, which provides a feasible recycling pathway of pyrite from mining tailings.

The customizability is another attractive characteristic of pyrite for AOPs. Apart

from natural pyrite, synthetic pyrite is used in some AOP studies. Synthetic pyrite typically serves as the substitution of natural pyrite for particular research requirement, such as specific size or purity. High-quality pyrite product can be obtained via simple hydrothermal reactions (Fig. 1b). Generally, ferrous sulfate ($FeSO_4$), sodium thiosulfate ($Na_2S_2O_3$), and sulfur (S) are used as the reactants. For example, in the FeS_2 synthesis process reported by Wang et al. (2020b), sulfur powder was added after $FeSO_4 \cdot 7H_2O$ and $Na_2S_2O_3$ were dissolved in water, and then the resulting suspension was fully stirred and transferred to an autoclave for conducting the hydrothermal reaction. The overall reaction can be described as the Eq. (3). The artificially synthesized FeS_2 is similar to natural pyrite, and it is convenient to adjust and control the properties. Besides the hydrothermal synthesis method, many other methods such as hot injection method, template-directed synthesis, and direct thermal sulfidation can also be used to synthesize FeS_2 (Trinh et al. 2017; Qin et al. 2018). Though these methods are all available, the hydrothermal synthesis is recommended to prepare amounts of FeS_2 for large-scale applications in AOPs due to its relatively simpler apparatus and technique. Compared with natural pyrite, synthetic pyrite with high purity is more suitable for the research of related mechanisms.

$$FeSO_4 + Na_2S_2O_3 + S + H_2O \rightarrow FeS_2 + Na_2SO_4 + H_2SO_4 \quad (3)$$

3. Application of pyrite-mediated AOPs for treating refractory organic pollutants

Pyrite has been shown to successfully function in various AOPs, mainly including

Fenton oxidation, electro-Fenton oxidation, and persulfate oxidation processes. In this section, the performance of pyrite-mediated AOPs in organic wastewater treatment is presented and the basic mechanisms are discussed and illustrated.

3.1. Pyrite-mediated Fenton oxidation processes

Fenton oxidation is a classical chemical reaction named with its discoverer Henry John Horstman Fenton (Koppenol 1993). This reaction generates hydroxyl radical (·OH) with strong oxidizing capacity from hydrogen peroxide (H_2O_2) and ferrous ion (Fe^{2+}), and the basic process is represented by the Eq. (4). The redox potential of the strong oxidizer ·OH reaches up to 2.80 V, which is next only to fluorine (Mousset et al. 2017). Therefore, Fenton oxidation is powerful in mineralizing various organic pollutants, especially some refractory aromatic compounds and heterocyclic compounds. Significantly, Fenton reaction is generally effective in acidic condition as the precipitation of dissolved iron species will occur in the solution with a high pH value (Jung et al. 2009). In the application of Fenton reaction for degrading organic pollutants, ferrous salts (e.g., ferrous sulfate) are often used as the iron source. Using pyrite to substitute ferrous salts can also trigger the Fenton reaction and achieve effective removal of organic pollutants in wastewater (Table 1). For example, Zhang et al. (2014b) prepared natural pyrite catalyst by simple grinding method and used it to catalyze the Fenton reaction for nitrobenzene degradation in the aqueous solution. According to their results, about 80% of the nitrobenzene was degraded within 300 min in the optimal conditions of 2.0 g/L of the catalyst, 250 mM of H_2O_2, 20 mg/L of initial nitrobenzene,

and a pH value of 3.0, while the classical Fenton system (with ferrous sulfate) could only remove 30% of the pollutant. The poor performance of classical Fenton system might be attributed to the early termination of the nitrobenzene degradation due to the Fe-sludge formation, which was overcome in pyrite Fenton system. On the one hand, the release of Fe^{2+} from pyrite is slow and the resulting Fe^{3+} can be reduced back to Fe^{2+} for Fenton reaction via its interaction with pyrite, which achieves the recycle of ferric ions. On the other hand, the pH-regulating ability of pyrite maintains an unfavourable acidic condition for Fe-sludge formation. Although pyrite showed high performance in Fenton degradation of many organics, the removal of total organic carbon (TOC) which indicates the absolute mineralization of organics varied with the targeted pollutants. Kantar et al. (2019b) applied pyrite Fenton system for removing chlorophenols, and their results showed that a significant portion of TOC still remained in the solution though all the chlorophenols were degraded within 40 min. The remained TOC mainly resulted from the formation of chlorinated organic intermediates and low-molecular-weight acids during the Fenton degradation process. Mashayekh-Salehi et al. (2021) used tetracycline as the targeted pollutant of their pyrite/H_2O_2 oxidation process, and the results suggested that the pollutant was completely degraded and over 85% could be mineralized within 60 min. These examples show promising potential of pyrite as a heterogeneous catalyst in Fenton oxidation for organic pollutant degradation. Similar to other heterogeneous catalysts, pyrite catalyst needs be used with suitable chemical reactors for practical applications of pyrite-mediated Fenton oxidation processes.

$$H_2O_2 + Fe^{2+} \rightarrow \cdot OH + Fe^{3+} + OH^- \quad (4)$$

The proposed mechanisms of pyrite-mediated Fenton oxidation processes are depicted in Fig. 2. The whole process involves three main phases: release of iron species from pyrite, generation of ·OH by Fenton reaction, degradation of organic pollutants by ·OH attack. The oxidative dissolution of pyrite by O_2 releases ferrous ions (Eq. (1)), which subsequently participate in the Fenton reaction. Besides ferrous ions, ferric ions may be generated via the oxidation of pyrite by H_2O_2 in the Fenton system (Eq. (5)) (Zhang et al. 2018b). The concomitant hydrogen ions during the release processes of iron species from pyrite effectively regulate the pH value of the Fenton system (Ltaïef et al. 2018). In the Fenton process, ·OH is generated from H_2O_2 while Fe^{2+} is oxidized to Fe^{3+} (Eq. (4)). The Fe^{3+} can be reduced back to Fe^{2+} (Fe^{2+}/Fe^{3+} cycle) via the process shown by Eq. (6), a rate-limiting step of Fenton process (Nichela et al. 2015). In the presence of pyrite, the regeneration of Fe^{2+} can also be achieved through the process represented by Eq. (2). As described by the equation, the interaction between pyrite and Fe^{3+} not only realizes the regeneration of Fe^{2+} from Fe^{3+} in the solution, but also promotes the release of Fe^{2+} from pyrite. Therefore, pyrite facilitates the Fe^{2+}/Fe^{3+} cycle in the Fenton process, and thus promotes the production of ·OH for the following oxidation degradation of organics. However, the relevance of pyrite dissolution to free radical production needs further research, and the sustainability of aforementioned mechanisms during the whole Fenton process waits to be verified.

$$2FeS_2 + 15H_2O_2 \rightarrow 2Fe^{3+} + 4SO_4^{2-} + 2H^+ + 14H_2O \quad (5)$$

$$Fe^{3+} + H_2O_2 \rightarrow Fe^{2+} + H^+ + HO_2^{\cdot} \quad (6)$$

3.2. Pyrite-mediated electro-Fenton oxidation processes

Based on the reaction mechanisms of classical Fenton oxidation, electro-Fenton oxidation utilizes electrochemically generated H_2O_2, instead of adscititious H_2O_2 reagent, to produce ·OH (He and Zhou 2017). The generation of H_2O_2 occurs on the cathode via two-electron reduction of O_2 under acidic condition (Eq. (7)). The supply of O_2 is generally made by aeration or O_2 injection (Li et al. 2020a). Additionally, the regeneration of Fe^{2+} can also be achieved through the cathodic reduction of Fe^{3+} in the solution (Eq. (8)). Compared with classical Fenton oxidation, the main advantages of electro-Fenton oxidation includes that: (1) the electrochemical generation of H_2O_2 avoid the safety risk of H_2O_2 reagent during its transportation, storage, and use; (2) the controllable degradation rate of pollutants favors the study of degradation process and mechanism; and (3) the continuous regeneration of Fe^{2+} reduces the Fe-sludge formation. Using pyrite as the heterogeneous electro-Fenton catalyst shows excellent performance for removing organic pollutants in wastewater (Table 2). In the electro-Fenton systems, pyrite mainly acts as the iron source in the electro-Fenton oxidation processes, which avoids the use of soluble iron salts or the loss of metal electrode in traditional electro-Fenton oxidation. Ammar et al. (2015) used natural pyrite to catalyze the electro-Fenton oxidation for removing tyrosol from wastewater, and they found that 89% TOC was reduced in 360 min under the conditions of 1.0 mg/L of pyrite catalyst, 300 mA of electric current, and 0.3 mmol/L of initial tyrosol. Additionally, pyrite can function as pH regulator and Fe^{3+} reductor to maintain long-time favorable reaction

conditions. A highlighted phenomenon during the electro-Fenton oxidation conducted by Ammar et al. (2015) was that pyrite could spontaneously regulate the solution pH to a suitable value of 2.8–3.7. Similar results were also found in using pyrite-mediated electro-Fenton oxidation to remove other organic pollutants such as levofloxacin, sulfamethazine, and diclofenac (Barhoumi et al. 2015, Barhoumi et al. 2016, Yu et al. 2020). Compared with direct use of pyrite as Fenton catalyst, the cases of using pyrite for electro-Fenton oxidation are less. This gives greater research space for exploring electrochemical applications of pyrite.

$$O_2 + 2H^+ + 2e^- \rightarrow H_2O_2 \quad (7)$$

$$Fe^{3+} + e^- \rightarrow Fe^{2+} \quad (8)$$

The proposed mechanisms of pyrite-mediated electro-Fenton oxidation processes are depicted in Fig. 3. The reduction of dissolved O_2 at the cathode produces H_2O_2 (Eq. (7)), while the oxidative dissolution of pyrite releases iron species (Eq. (1) and Eq. (5)). The released Fe^{2+} can directly participate in the Fenton reaction with H_2O_2 generated at the cathode. The Fe^{3+} both released from pyrite (via H_2O_2 oxidation) and generated from Fenton reaction can be reduced to Fe^{2+} via multiple pathways including pyrite reduction (Eq. (2)) and cathodic reduction (Eq. (8)). These processes facilitate the Fe^{2+}/Fe^{3+} cycle and promote the ·OH generation in electro-Fenton system. Various production processes of hydrogen ions (Eq. (1), Eq. (2), and Eq. (5)) support the spontaneous pH-regulation capacity of the pyrite/electro-Fenton system. Additionally, the water oxidation at a high-oxygen overvoltage anode produces supplementary ·OH and H^+ (Eq. (9)) (Nidheesh and Gandhimathi 2012). Continuous ·OH generation and

its facilitating processes provide potent oxidizing capacity for the degradation of organic pollutants. Few studies focused on the electrochemical characteristics of pyrite and non-radical degradation pathways of organics in pyrite-mediated electro-Fenton system. Future studies on these aspects may help to go deep into the mechanisms.

$$H_2O \rightarrow \cdot OH + H^+ + e^- \quad (9)$$

3.3. Pyrite-mediated persulfate oxidation processes

Conventional AOPs are based on the strong oxidizing capacity of ·OH, while persulfate oxidation technology utilizes sulfate radical ($SO_4^{\cdot-}$), a free radical with the strong oxidizing capacity close to ·OH, as the main active species to degrade organic pollutants (Oh et al. 2016). Persulfate includes peroxymonosulfate (PMS, HSO_5^-) and peroxydisulfate (PDS, $S_2O_8^{2-}$), and both of them contain peroxy bond (–O–O–) in their molecular structure. The cleaving of the peroxy bond in persulfate via energy and electron transfer reactions generates $SO_4^{\cdot-}$ with a high oxidation potential of 2.60 V (Tsitonaki et al. 2010). Compared with ·OH, $SO_4^{\cdot-}$ offers many more advantages in AOPs, including that: (1) $SO_4^{\cdot-}$ possesses a longer half-life time than that of ·OH (30–40 μs vs. <1 μs), which ensures it to attack the targeted pollutants more effectively; (2) $SO_4^{\cdot-}$ can react with organic pollutants in a broad pH range of 2.0–8.0; and (3) persulfate is safer than H_2O_2 during its transportation, storage, and use (Zhao et al. 2017, Xiao et al. 2020). Various methods can be applied to activate persulfate for produce $SO_4^{\cdot-}$, such as thermal activation, alkaline activation, radiation activation, transition metal activation, and carbonaceous material activation (Wang and Wang 2018). Using

pyrite to provide ferrous ions can effectively activate persulfate and produce strong oxidizer $SO_4^{\cdot -}$ for removing organic pollutants in wastewater (Table 3), and the activating processes can be expressed as Eqs. (10) and (11) (Zhang et al. 2014a, Ali et al. 2021). For example, Li et al. (2021) used pyrite/PMS system for degrading propanil, and they found that 91.9% of the propanil could be degraded within 15 min under the optimal conditions and $SO_4^{\cdot -}$ and ·OH are the dominant reactive species. Chen et al. (2018) used ethylthionocarbamate as the targeted pollutant of their pyrite/PDS oxidation process, and the results suggested that 96.64% of the pollutant was degraded within 180 min and $SO_4^{\cdot -}$ functioned as the predominant reactive species. Rahimi et al. (2021) prepared pyrite nanoparticles with a ball mill by using mine waste as the raw material, and applied them as the catalysts to activate PMS and PDS for tetracycline degradation. According to their results, the removal rate of tetracycline in PDS and PMS system was respectively 32.5% and 98.7% within 30 min under the conditions of 1.0 mg/L of pyrite, 1.0 g/L of PDS/PMS, 50 mg/L of initial tetracycline, and an initial pH value of 4.1. Compared with PDS, PMS could be more effectively activated by pyrite, which might be attributed to the asymmetric structure of PMS molecular (Song et al. 2020).

$$Fe^{2+} + HSO_5^- \rightarrow Fe^{3+} + SO_4^{\cdot -} + OH^- \quad (10)$$

$$Fe^{2+} + S_2O_8^{2-} \rightarrow Fe^{3+} + SO_4^{\cdot -} + SO_4^{2-} \quad (11)$$

The proposed mechanisms of pyrite-mediated persulfate oxidation processes are depicted in Fig. 4. Besides the oxidative dissolution of pyrite by O_2 (Eq. (1)), pyrite releases iron ions via the oxidation effect of persulfate, and the oxidation process by

PMS and PDS can be expressed by Eqs. (12) and (13) (Liang et al. 2010, Feng et al. 2018). The released Fe^{2+} activates the PMS and PDS to generate $SO_4\cdot^-$ by the pathways represented by Eqs. (10) and (11). In addition to the above pathways, $SO_4\cdot^-$ may be generated via direct pyrite oxidation by PMS and PDS (Eqs. (14) and (15)) (Rahimi et al. 2021). By the attack of $SO_4\cdot^-$, the targeted organics can be effectively degraded. During the oxidation process, the regeneration of Fe^{2+} from Fe^{3+} and the release of Fe^{2+} from pyrite can be promoted via the reaction between Fe^{3+} and pyrite (Eq. (2)), thus facilitating the Fe^{2+}/Fe^{3+} cycle and the $SO_4\cdot^-$ production. In the pyrite/persulfate systems, ·OH may generate via $SO_4\cdot^-$, and the processes are represented by Eqs. (16) and (17) (Ismail et al. 2017). Both $SO_4\cdot^-$ and the concomitant ·OH can function to degrade organic pollutants. In the aqueous solution, excessive Fe^{2+} will consume the functional $SO_4\cdot^-$ and ·OH (Eqs. (18) and (19)) (Shang et al. 2019). The slow release of Fe^{2+} from pyrite avoids the unwanted consumption of these free radicals, which ensures the high-efficiency oxidation capacity of the pyrite-mediated persulfate oxidation processes (Liang et al. 2010). Additionally, sulfur species play an important role in the activated oxidation by pyrite. Different valence states of sulfur, including monosulfide (S^{2-}), disulfide (S_2^{2-}), polysulfide (S_n^{2-}), elemental sulfur (S^0), and sulfate (SO_4^{2-}), were present in pyrite oxidation systems, and the reductive low-valence sulfur importantly function in the Fe^{2+}/Fe^{3+} cycle (He et al. 2021). Zhou et al. (2018) highlighted the role of sulfide as electron donors for PMS activation, and reported that although the Fe^{2+} on pyrite efficiently activated PMS, the Fe^{2+} regeneration and subsequent PMS activation were crucially controlled by S_2^{2-}. More mechanism studies from the point of sulfur

species are expected to improve the understanding of pyrite-mediated persulfate oxidation, as both pyrite and persulfate can release sulfur species into the solution during the oxidation process.

$$FeS_2 + 7HSO_5^- + H_2O \rightarrow Fe^{2+} + 9SO_4^{2-} + 9H^+ \quad (12)$$

$$2FeS_2 + 15S_2O_8^{2-} + 16H_2O \rightarrow 2Fe^{3+} + 34SO_4^{2-} + 32H^+ \quad (13)$$

$$2HSO_5^- + FeS_2 \rightarrow 2SO_4^{\cdot -} + 2OH^- + Fe^{2+} + 2S \quad (14)$$

$$2S_2O_8^{2-} + FeS_2 \rightarrow 2SO_4^{\cdot -} + 2SO_4^{2-} + Fe^{2+} + 2S \quad (15)$$

$$SO_4^{\cdot -} + H_2O \rightarrow SO_4^{2-} + \cdot OH + H^+ \quad (16)$$

$$SO_4^{\cdot -} + OH^- \rightarrow SO_4^{2-} + \cdot OH \quad (17)$$

$$Fe^{2+} + SO_4^{\cdot -} \rightarrow Fe^{3+} + SO_4^{2-} \quad (18)$$

$$Fe^{2+} + \cdot OH \rightarrow Fe^{3+} + OH^- \quad (19)$$

3.4. Others

In addition to the above-mentioned AOP applications, some researchers have tried to use pyrite in calcium peroxide (CaO_2) oxidation, photocatalytic oxidation, and ozone oxidation for degrading organic pollutants. Considering the safety risk and instability of liquid H_2O_2 reagent, Zhou et al. (2020) used solid CaO_2 as the H_2O_2 source, and applied the pyrite/CaO_2 system to degrade diethyl phthalate based on the Fenton oxidation mechanism. Their experimental results suggested that 10 mg/L of diethyl phthalate could be completely degraded by the pyrite/CaO_2 system within 5.0 min at a pH value of 3.5. Diao et al. (2015) applied natural pyrite as photocatalyst for degrading malachite green with ultraviolet irradiation. In the photocatalytic experiment, 1.0 g/L

of pyrite could degrade 96.7% of the malachite green within 120 min via a photo-Fenton like process. Wu et al. (2016b) used pyrite as an ozonation catalyst for degrading reactive black 5, and the mineralization efficiency increased by 17.39% compared with using ozone alone. The ·OH generated by the reaction between ozone and pyrite surface was considered the main mechanism. Involving pyrite into other AOP systems is now under active exploration, and interesting and meaningful results will further expand the application scope and development prospect of pyrite in AOP systems.

4. Enhancing strategies of pyrite-mediated AOPs

Although many pyrite-mediated AOP systems have been successfully developed for organic wastewater treatment, some strategies are proposed (Fig. 5) as researchers always make perfection more perfect when developing new catalysts. They are proposed to further enhance the performance or overcome the limitations such as insufficient surface reactivity of pyrite, slow pyrite dissolution, limited efficiency of heterogeneous reactions on the solid-liquid interface, and low catalytic activity of pyrite under high pH conditions. These enhancing strategies are also suitable for some other activation systems, and they were referred or adopted by the researchers for enhancing the performance of pyrite-mediated AOPs. In this section, the introduced enhancing strategies were used and supported with at least one research paper.

4.1. Making pyrite into nanoparticles

In order to overcome the insufficient surface reactivity of pyrite in some AOP

systems, making pyrite into nanoparticles is proposed. This strategy has the advantage of improving the catalytic activity of pyrite in AOPs. Nanoparticles are small particles with dimensions in a nanoscale range (1–100 nm). Compared with conventional materials, nanoparticles typically have higher specific surface area and surface energy, which offers greater chemical reactivity (Santos et al. 2015). In laboratory experiments, natural pyrite is generally ground into nanoparticles by a ball mill (Mashayekh-Salehi et al. 2021, Rahimi et al. 2021), while synthetic pyrite nanoparticles can be obtained through the control of synthesis conditions (Qin et al. 2018). Gil-Lozano et al. (2014) compared the efficacy of pyrite microparticles (1.4 μm) and pyrite nanoparticles (20 nm) in catalyzing Fenton degradation of copper phthalocyanine, and the two particles could remove 7% and 60% of the pollutant at the same low dosage of 0.08 mg/L, respectively. However, this strategy is too difficult to be practical at the present time. Innovations in the production equipment of pyrite nanoparticles and chemical reactor of nanomaterials are needed to achieve the practical application.

4.2. Assisting by ultrasound

Considering the limited efficiency of heterogeneous reactions on the solid-liquid interface, the combination of pyrite-mediated AOPs and ultrasound has received interest from researchers to enhance the catalytic performance. The advantages of ultrasound assistance in pyrite-mediated AOPs mainly include refreshing the pyrite surface, producing additional active free radicals, and facilitating the mass transfer. In the aqueous solution, continuous ultrasonic wave can help to clean and refresh the

394 pyrite surface by peeling off the oxide layer and pitting the pyrite surface (Gao et al.
395 2018). Additional active free radicals (e.g., ·OH, ·H, HO_2·, and ·O_2^-) may be produced
396 during the ultrasonic treatment by triggering acoustic cavitation which involves the
397 formation, rapid growth, and violent collapse of cavitation bubbles (Zhang et al. 2018a).
398 Additionally, the strong mechanical effect generated by ultrasound can enhance the
399 mass transfer at solid-liquid interface (Guo et al. 2017). Diao et al. (2020) coupled
400 ultrasound with pyrite/PMS system for the degradation of 2,4-dichlorophenol, and their
401 results showed that the degradation efficiency increased from 71.3% to 97.9% with the
402 assistance of ultrasonic treatment. This result demonstrates the effectiveness of
403 ultrasound for assisting the activation process of pyrite-mediated AOPs.
404
405 4.3. Enhancing by light irradiation
406 Similar to the ultrasonic assistance, light irradiation can help to enhance the
407 performance of pyrite-mediated AOPs by taking the advantage of the semiconductor
408 characteristics of pyrite. The suitable band gap (direct: 1.03 eV; indirect: 0.95 eV) and
409 high optical absorption coefficient (10^5 cm^{-1} for hν > 1.3 eV) enable pyrite to absorb
410 light and generate electron (e^-) and hole (h^+) under light irradiation (Morales-Gallardo
411 et al. 2016). The photo-induced carriers can react with the components such as pyrite,
412 Fe^{3+}, H_2O, and O_2 in AOP systems, thus facilitating the production of reactive oxidative
413 species (Vorontsov 2019). Using light irradiation for assistance can effectively improve
414 the catalytic activity of pyrite in AOPs. For example, Zeng et al. (2019) used visible
415 light to enhance the pyrite-mediated Fenton oxidation process for *p*-nitrophenol

degradation, and the complete degradation time was shortened from 10 min to 4 min with the assistance of visible light irradiation. However, using light irradiation for assistance is technically difficult to achieve in practical applications as the effective optical path in current reactor for pyrite-mediated advanced oxidation would be very small.

4.4. Adding exogenous ferric ions

Although pyrite-mediated AOPs show excellent application prospects, it suffers from low reaction rate and excessive H_2O_2 is usually needed to shorten reaction time. The production of Fe^{2+} is the rate-determining step in pyrite-mediated AOPs. Considering that the generation of Fe^{2+} from oxidizing pyrite by Fe^{3+} is much faster than that from oxidizing pyrite by O_2, exogenous Fe^{3+} can help to overcome the slow pyrite dissolution and accelerate the Fe^{2+} generation, thereby enhancing the degradation performance of pyrite-mediated AOPs. Wu et al. (2015) investigated the effect of Fe^{3+} on pyrite oxidation in the Fenton system, and they found that the final solution pH decreased from 3.02 to 2.91 with the increasing concentration of added Fe^{3+} and the oxidative degradation efficiency of chloramphenicol by the system was significantly reduced from 100% to less than 30% by adding 0.5 mM of phosphate buffer as Fe^{3+} chelating agent.

4.5. Chelating iron ions by organic ligands

Under high pH condition, the iron precipitation significantly inhibits the catalytic

activity of pyrite in AOP systems, which limits the pH range of applications. Adding organic chelating agents is proposed to enhance the catalytic performance, as organic chelating agents can inhibit the precipitation of iron ions, especially at a relatively high pH condition, by acting as a ligand to form chelate compounds with iron ions (Bai et al. 2021). This is conducive to extending the application pH range of pyrite-mediated AOPs. Additionally, the chelating effects of organic ligands could help to induce the generation of Fe^{2+} from pyrite surface and facilitate the Fe^{2+}/Fe^{3+} cycle. Wu et al. (2016a) used as a biodegradable chelating agent, tetrasodium glutamate diacetate (GLDA), successfully enhanced the performance of pyrite-mediated Fenton oxidation for chloramphenicol degradation at a pH value of 8.0, and they found that GLDA increased the ·OH production and GLDA-chelated Fe^{2+} accelerated the Fe^{2+}/Fe^{3+} cycle. Similarly, Kantar et al. (2019a) used citrate to enhance the performance of treating pharmaceutical wastewater by a continuous flow pyrite/H_2O_2 systems. Their results showed that the TOC removal in the presence of citrate was much higher than that without citrate, and the increased iron dissolution and reduced column clogging by citrate were considered the main causes.

4.6. Accelerating oxidation by biochar

Although pyrite can promote the Fe^{2+}/Fe^{3+} cycle in AOPs, the insufficient Fe^{2+} regeneration and low heterogeneous reaction rate may impeded the sustainability of high efficiency of pyrite-mediated AOPs during the whole oxidation process. Recent research enthusiasm on biochar offers a new strategy to address this issue. Biochar is a

porous pyrolysis products of biomass materials, and it has been extensively applied in environmental remediation by reason of its high adsorption capacity for many pollutants, positive role as electron transfer mediator, and various persistent free radicals (Luo et al. 2021). These characteristics are also favorable for organic pollutant degradation by pyrite-mediated AOPs. Biochar can concentrate organic pollutants at solid-liquid interface by adsorption, which facilitates their catalytic degradation. The electron transfer capacity and persistent free radicals benefit the free radical generation and the Fe^{2+}/Fe^{3+} cycle. Zhu et al. (2020) added biochar to the pyrite/H_2O_2 system for accelerating the degradation of 2,4-dichlorophenoxyacetic acid, and the degradation rate constant was 1.98–2.39 times higher with the addition of 0.1 g/L of biochar.

5. Summary of pyrite advantages for AOPs

Pyrite is an attractive catalyst for advanced oxidation reactions in recent studies, as it has many advantages compared with other catalyst materials (Fig. 6 and Table 4). Pyrite is a plentiful natural mineral on earth, which offers a rich source for the catalyst materials. For example, the newly-discovered reserves of pyrite in China reached 68.62 million tons in 2019 (Ministry of Natural Resources 2020). Using pyrite as the catalyst is cost effective. Compared with metal catalysts, especially noble metal, pyrite is much cheaper, and it can often be obtained from the recycling of mine tailings (Schellenbach and Krekeler 2012, Lü et al. 2018). Current market price of pyrite is reported as cheap as $100–300/ton (Li et al. 2016, Hu et al. 2020), which shows competitive price advantage. Solid pyrite plays a positive role in heterogeneous catalysis. The solid state

of pyrite facilitates the catalyst separation from the reaction system, the catalyst reuse in practical application, and the control of possible pollution caused by metal ions (Yu et al. 2020). The oxidative dissolution of pyrite in aqueous solution slowly releases ferrous ions. Constantin and Chiriţă (2013) investigated the oxidative dissolution of pyrite in acidic media (pH 2.5 and 25 °C) and found that the dissolution rates of pyrite by O_2 (saturated), H_2O_2 (0.1 M), and Fe^{3+} (0.01 M) were 2.53×10^{-4}, 1.52×10^{-2}, and 9.35×10^{-2} μmol/m^2/s, respectively. Thus, using pyrite as a sustainable iron source to drive advanced oxidation reactions can obviate using soluble iron salts and forming iron sludge. Peng et al. (2017) reported that the iron sludge production of their electro-Fenton treatment could reach 1.19 to 3.23 kg/m^3 after 60 min. The undesired iron sludge production can be inhibited or eliminated due to the Fe^{2+}/Fe^{3+} cycle and the self-regulated acidic condition in pyrite-mediated electro-Fenton system (Yu et al. 2020). Apart from ferrous ions, the oxidative dissolution of pyrite simultaneously produces hydrogen ions, conducive to maintaining a favorable acidic condition for advanced oxidation reactions (Wu et al. 2015, Ltaïef et al. 2018). Both the structural ferrous ion and the reductive sulfide species in pyrite can participate in redox reactions via acting as electron donors. These reductive species can support multiple functions at the same time, such as activating persulfate and reducing pollutant (He et al. 2021). These characteristics of pyrite make it competitive as a multifunction catalyst because amounts of pollutants are hard to be oxidized by conventional wastewater treatments. Additionally, the easy processing technologies and the environmentally friendly feature are also attractive points of pyrite catalyst (Fathinia et al. 2015). These advantages

encourage the use of pyrite as a low-cost heterogeneous catalyst in AOPs.

However, natural pyrite often serves as a sink for some toxic trace metals, such as lead, zinc, cadmium, arsenic, and copper (Tabelin et al. 2018). These accompanying elements may be released during pyrite oxidation. Although their concentrations are very small, the risk of these toxic elements during wastewater treatment should be noted. Reasonable classification and management of pyrite raw materials based on the source and advance leaching test is recommended to ensure that the benefits of pyrite in AOPs outweigh the risks.

6. Conclusions and outlook

In summary, pyrite can be an excellent catalyst for AOPs including Fenton oxidation, electro-Fenton oxidation, and persulfate oxidation processes, and pyrite-mediated AOP systems show great application prospect in treating organic wastewater. Natural pyrite is an abundant low-cost heterogeneous catalyst for AOPs, and the slow release of Fe^{2+} and the self-regulation of solution pH are highlighted characteristics of pyrite-mediated AOPs. Synthetic pyrite typically serves as the substitution of natural pyrite for particular research requirement. In AOPs, pyrite slowly releases Fe^{2+} to trigger the advanced oxidation reactions. The interaction between Fe^{3+} and pyrite facilitates the Fe^{2+} regeneration and the Fe^{2+}/Fe^{3+} cycle in AOPs. Making pyrite into nanoparticles, assisting by ultrasound and light irradiation, and adding exogenous Fe^{3+}, organic chelating agents, or biochar is effective to further enhance the performance of pyrite-mediated AOPs.

In the future, the research priority on this topic should be given to the following issues. The first is the potential risks of pyrite in AOP systems. Besides the main component FeS_2, natural pyrite may contain some accompanying elements such as nickel, cobalt, copper, arsenic, selenium, gold, and silver. Whether these toxic trace elements cause toxic effects through the treating processes of pyrite-mediated AOPs or not is worth exploring. Before the practical application, confirming this point is necessary to avoid unintended consequences of pyrite-mediated AOPs. Therefore, toxicity research on pyrite and its oxidation solution is needed. The second is the mechanisms of pyrite-mediated AOPs. The current research is mainly from the points of active oxidative species and pollutant degradation pathways. Further mechanism research may consider the synchronous changes of pyrite, such as the surface oxidation during pyrite-mediated AOPs. Illuminating the relationship between the oxidation degree of pyrite and its catalytic activity will help to optimize the technological processes of pyrite storage, pretreatment, and application. The third is about the application research mainly including the technological coupling, practical wastewater treatment, and equipment development. Direct use of pyrite-mediated AOPs for industrial wastewater treatment may be difficult and high-cost. Thus, coupling pyrite-mediated AOPs with conventional biological methods might be more suitable for it to reach practical application. Applying pyrite-mediated AOPs as a pretreatment step of conventional biological methods can enhance the biodegradability, especially for refractory organics with less bioavailability. The components of practical industrial wastewater are complicated, and various factors (e.g., high salinity, high TOC content,

and coexistence of multiple pollutants) significantly affect the removal efficiency of targeted pollutants. Therefore, the effectiveness of pyrite-mediated AOPs for treating practical organic wastewater should be further confirmed according to the characteristics of wastewater from different industries. Additionally, current studies on pyrite-mediated AOPs are mostly at the stage of laboratory research, the water treatment capacity is limited, and the cost and corrosion problems of the equipment are often not considered. In the future studies, designing simple, high-efficiency, and reliable reactors for practical application of pyrite-mediated AOPs is recommended.

Acknowledgements

This work was supported by the National Natural Science Foundation of China (U20A20323, 82003363, 52100180, 51521006), the China National Postdoctoral Program for Innovative Talents (BX20200119), the Project funded by China Postdoctoral Science Foundation (2021M690961), the Hunan Provincial Natural Science Foundation of China (2021JJ40087, 2021JJ40820), and the Changsha Municipal Natural Science Foundation (kq2007059).

References

Abraitis, P.K., Pattrick, R.A.D. and Vaughan, D.J. (2004) Variations in the compositional, textural and electrical properties of natural pyrite: a review. International Journal of Mineral Processing 74(1), 41-59.

Ali, J., Shahzad, A., Wang, J., Ifthikar, J., Lei, W., Aregay, G.G., Chen, Z. and Chen, Z. (2021) Modulating the redox cycles of homogenous Fe(III)/PMS system through constructing electron rich thiomolybdate centres in confined layered double hydroxides. Chemical Engineering Journal 408, 127242.

Ammar, S., Oturan, M.A., Labiadh, L., Guersalli, A., Abdelhedi, R., Oturan, N. and Brillas, E. (2015) Degradation of tyrosol by a novel electro-Fenton process using pyrite as heterogeneous source of iron catalyst. Water Research 74, 77-87.

Asgari, E., Mohammadi, F., Nourmoradi, H., Sheikhmohammadi, A., Rostamifasih, Z., Hashemzadeh, B. and Arfaeinia, H. (2020) Heterogeneous catalytic degradation of nonylphenol using persulphate activated by natural pyrite: response surface methodology modelling and optimisation. International Journal of Environmental Analytical Chemistry, 1-20.

Bagnato, G., Boulet, F. and Sanna, A. (2019) Effect of Li-LSX zeolite, NiCe/Al_2O_3 and NiCe/ZrO_2 on the production of drop-in bio-fuels by pyrolysis and hydrotreating of *Nannochloropsis* and *isochrysis* microalgae. Energy 179, 199-213.

Bai, Y., Wu, D., Wang, W., Chen, P., Tan, F., Wang, X., Qiao, X. and Wong, P.K. (2021) Dramatically enhanced degradation of recalcitrant organic contaminants in MgO_2/Fe(III) Fenton-like system by organic chelating agents. Environmental

Research 192, 110242.

Barhoumi, N., Labiadh, L., Oturan, M.A., Oturan, N., Gadri, A., Ammar, S. and Brillas, E. (2015) Electrochemical mineralization of the antibiotic levofloxacin by electro-Fenton-pyrite process. Chemosphere 141, 250-257.

Barhoumi, N., Oturan, N., Ammar, S., Gadri, A., Oturan, M.A. and Brillas, E. (2017) Enhanced degradation of the antibiotic tetracycline by heterogeneous electro-Fenton with pyrite catalysis. Environmental Chemistry Letters 15(4), 689-693.

Barhoumi, N., Oturan, N., Olvera-Vargas, H., Brillas, E., Gadri, A., Ammar, S. and Oturan, M.A. (2016) Pyrite as a sustainable catalyst in electro-Fenton process for improving oxidation of sulfamethazine. Kinetics, mechanism and toxicity assessment. Water Research 94, 52-61.

Boczkaj, G. and Fernandes, A. (2017) Wastewater treatment by means of advanced oxidation processes at basic pH conditions: A review. Chemical Engineering Journal 320, 608-633.

Bulut, G., Yenial, Ü., Emiroğlu, E. and Sirkeci, A.A. (2014) Arsenic removal from aqueous solution using pyrite. Journal of Cleaner Production 84, 526-532.

Cai, F., Lei, L., Li, Y. and Chen, Y. (2021) A review of aerobic granular sludge (AGS) treating recalcitrant wastewater: Refractory organics removal mechanism, application and prospect. Science of The Total Environment 782, 146852.

Chandra, A.P. and Gerson, A.R. (2010) The mechanisms of pyrite oxidation and leaching: A fundamental perspective. Surface Science Reports 65(9), 293-315.

Chen, S., Xiong, P., Zhan, W. and Xiong, L. (2018) Degradation of

ethylthionocarbamate by pyrite-activated persulfate. Minerals Engineering 122, 38-43.

Constantin, C.A. and Chiriţă, P. (2013) Oxidative dissolution of pyrite in acidic media. Journal of Applied Electrochemistry 43(7), 659-666.

Demiya, M., Uddin, M.A. and Kato, Y. (2018) Enhancement in trichloroethylene dechlorination by mixed particles of iron–iron disulfide or iron–iron sulfide. Journal of Environmental Chemical Engineering 6(1), 1020-1026.

Diao, Z.H., Lin, Z.Y., Chen, X.Z., Yan, L., Dong, F.X., Qian, W., Kong, L.J., Du, J.J. and Chu, W. (2020) Ultrasound-assisted heterogeneous activation of peroxymonosulphate by natural pyrite for 2,4-dichlorophenol degradation in water: Synergistic effects, pathway and mechanism. Chemical Engineering Journal 389, 123771.

Diao, Z.H., Liu, J.J., Hu, Y.X., Kong, L.J., Jiang, D. and Xu, X.R. (2017) Comparative study of Rhodamine B degradation by the systems pyrite/H_2O_2 and pyrite/persulfate: Reactivity, stability, products and mechanism. Separation and Purification Technology 184, 374-383.

Diao, Z.H., Xu, X.R., Liu, F.M., Sun, Y.X., Zhang, Z.W., Sun, K.F., Wang, S.Z. and Cheng, H. (2015) Photocatalytic degradation of malachite green by pyrite and its synergism with Cr(VI) reduction: Performance and reaction mechanism. Separation and Purification Technology 154, 168-175.

Fang, Y., Cao, X., Feng, W., Zhou, W., Johnson, D. and Huang, Y. (2020) High catalytic hydrolysis of microcystins on pyrite surface. Environmental Chemistry Letters 18(2),

483-487.

Fathinia, S., Fathinia, M., Rahmani, A.A. and Khataee, A. (2015) Preparation of natural pyrite nanoparticles by high energy planetary ball milling as a nanocatalyst for heterogeneous Fenton process. Applied Surface Science 327, 190-200.

Feng, J., Tian, H., Huang, Y., Ding, Z. and Yin, Z. (2019) Pyrite oxidation mechanism in aqueous medium. Journal of the Chinese Chemical Society 66(4), 345-354.

Feng, Y., Li, H., Lin, L., Kong, L., Li, X., Wu, D., Zhao, H. and Shih, K. (2018) Degradation of 1,4-dioxane via controlled generation of radicals by pyrite-activated oxidants: Synergistic effects, role of disulfides, and activation sites. Chemical Engineering Journal 336, 416-426.

Gao, Y., Gao, N., Wang, W., Kang, S., Xu, J., Xiang, H. and Yin, D. (2018) Ultrasound-assisted heterogeneous activation of persulfate by nano zero-valent iron (nZVI) for the propranolol degradation in water. Ultrasonics Sonochemistry 49, 33-40.

Gao, Y., Luo, J., Song, T. and Yu, X. (2021) Research progress on nano-Fe^0/PS system for degradation of refractory organics in aqueous solution. Journal of Environmental Chemical Engineering 9(4), 105345.

Gil-Lozano, C., Losa-Adams, E., F.-Dávila, A. and Gago-Duport, L. (2014) Pyrite nanoparticles as a Fenton-like reagent for in situ remediation of organic pollutants. Beilstein Journal of Nanotechnology 5, 855-864.

Grandclément, C., Seyssiecq, I., Piram, A., Wong-Wah-Chung, P., Vanot, G., Tiliacos, N., Roche, N. and Doumenq, P. (2017) From the conventional biological wastewater treatment to hybrid processes, the evaluation of organic micropollutant removal: A

review. Water Research 111, 297-317.

Gregory, D.D. and Kohn, M.J. (2020) Pyrite: Fool's gold records starvation of bacteria. American Mineralogist 105(2), 282-283.

Guo, J., Zhu, L., Sun, N. and Lan, Y. (2017) Degradation of nitrobenzene by sodium persulfate activated with zero-valent zinc in the presence of low frequency ultrasound. Journal of the Taiwan Institute of Chemical Engineers 78, 137-143.

Gwenzi, W. and Chaukura, N. (2018) Organic contaminants in African aquatic systems: Current knowledge, health risks, and future research directions. Science of The Total Environment 619-620, 1493-1514.

He, H. and Zhou, Z. (2017) Electro-Fenton process for water and wastewater treatment. Critical Reviews in Environmental Science and Technology 47(21), 2100-2131.

He, P., Zhu, J., Chen, Y., Chen, F., Zhu, J., Liu, M., Zhang, K. and Gan, M. (2021) Pyrite-activated persulfate for simultaneous 2,4-DCP oxidation and Cr(VI) reduction. Chemical Engineering Journal 406, 126758.

Herget, K., Hubach, P., Pusch, S., Deglmann, P., Götz, H., Gorelik, T.E., Gural'skiy, I.y.A., Pfitzner, F., Link, T., Schenk, S., Panthöfer, M., Ksenofontov, V., Kolb, U., Opatz, T., André, R. and Tremel, W. (2017) Haloperoxidase Mimicry by CeO_{2-x} Nanorods Combats Biofouling. Advanced Materials 29(4), 1603823.

Hu, Y., Wu, G., Li, R., Xiao, L. and Zhan, X. (2020) Iron sulphides mediated autotrophic denitrification: An emerging bioprocess for nitrate pollution mitigation and sustainable wastewater treatment. Water Research 179, 115914.

Ismail, L., Ferronato, C., Fine, L., Jaber, F. and Chovelon, J.M. (2017) Elimination of

sulfaclozine from water with SO_4^- radicals: Evaluation of different persulfate activation methods. Applied Catalysis B: Environmental 201, 573-581.

Jung, Y.S., Lim, W.T., Park, J.Y. and Kim, Y.H. (2009) Effect of pH on Fenton and Fenton-like oxidation. Environmental Technology 30(2), 183-190.

Kantar, C., Oral, O. and Oz, N.A. (2019a) Ligand enhanced pharmaceutical wastewater treatment with Fenton process using pyrite as the catalyst: Column experiments. Chemosphere 237, 124440.

Kantar, C., Oral, O., Urken, O., Oz, N.A. and Keskin, S. (2019b) Oxidative degradation of chlorophenolic compounds with pyrite-Fenton process. Environmental Pollution 247, 349-361.

Koppenol, W.H. (1993) The centennial of the Fenton reaction. Free Radical Biology and Medicine 15(6), 645-651.

Lü, C., Wang, Y., Qian, P., Liu, X., Fu, G., Ding, J., Ye, S. and Chen, Y. (2018) Separation of chalcopyrite and pyrite from a copper tailing by ammonium humate. Chinese Journal of Chemical Engineering 26(9), 1814-1821.

Labiadh, L., Oturan, M.A., Panizza, M., Hamadi, N.B. and Ammar, S. (2015) Complete removal of AHPS synthetic dye from water using new electro-fenton oxidation catalyzed by natural pyrite as heterogeneous catalyst. Journal of Hazardous Materials 297, 34-41.

Li, D., Zheng, T., Liu, Y., Hou, D., Yao, K.K., Zhang, W., Song, H., He, H., Shi, W., Wang, L. and Ma, J. (2020a) A novel Electro-Fenton process characterized by aeration from inside a graphite felt electrode with enhanced electrogeneration of

H_2O_2 and cycle of Fe^{3+}/Fe^{2+}. Journal of Hazardous Materials 396, 122591.

Li, R., Morrison, L., Collins, G., Li, A. and Zhan, X. (2016) Simultaneous nitrate and phosphate removal from wastewater lacking organic matter through microbial oxidation of pyrrhotite coupled to nitrate reduction. Water Research 96, 32-41.

Li, T., Abdelhaleem, A., Chu, W. and Xu, W. (2021) Efficient activation of oxone by pyrite for the degradation of propanil: Kinetics and degradation pathway. Journal of Hazardous Materials 403, 123930.

Li, W., Yang, S., Wang, W., Liu, Q., He, J., Li, B., Cai, Z., Chen, N., Fang, H. and Sun, S. (2020b) Simultaneous removal of Cr(VI) and acid orange 7 from water in pyrite-persulfate system. Environmental Research 189, 109876.

Li, Y., Tian, X., Liang, J., Chen, X., Ye, J., Liu, Y., Liu, Y. and Wei, Y. (2020c) Remediation of hexavalent chromium in contaminated soil using amorphous iron pyrite: Effect on leachability, bioaccessibility, phytotoxicity and long-term stability. Environmental Pollution 264, 114804.

Liang, C., Guo, Y.Y., Chien, Y.C. and Wu, Y.J. (2010) Oxidative degradation of MTBE by pyrite-activated persulfate: Proposed reaction pathways. Industrial & Engineering Chemistry Research 49(18), 8858-8864.

Liu, W., Wang, Y., Ai, Z. and Zhang, L. (2015) Hydrothermal synthesis of FeS_2 as a high-efficiency fenton reagent to degrade alachlor via superoxide-mediated Fe(II)/Fe(III) cycle. ACS Applied Materials & Interfaces 7(51), 28534-28544.

Liu, Z., Gao, Z. and Wu, Q. (2021) Activation of persulfate by magnetic zirconium-doped manganese ferrite for efficient degradation of tetracycline. Chemical

Engineering Journal 423, 130283.

Ltaïef, A.H., Pastrana-Martínez, L.M., Ammar, S., Gadri, A., Faria, J.L. and Silva, A.M. (2018) Mined pyrite and chalcopyrite as catalysts for spontaneous acidic pH adjustment in Fenton and LED photo-Fenton-like processes. Journal of Chemical Technology & Biotechnology 93(4), 1137-1146.

Luo, K., Pang, Y., Wang, D., Li, X., Wang, L., Lei, M., Huang, Q. and Yang, Q. (2021) A critical review on the application of biochar in environmental pollution remediation: Role of persistent free radicals (PFRs). Journal of Environmental Sciences 108, 201-216.

Ma, D., Yi, H., Lai, C., Liu, X., Huo, X., An, Z., Li, L., Fu, Y., Li, B., Zhang, M., Qin, L., Liu, S. and Yang, L. (2021) Critical review of advanced oxidation processes in organic wastewater treatment. Chemosphere 275, 130104.

Mashayekh-Salehi, A., Akbarnejad, K., Roudbari, A., Peter van der Hoek, J., Nabizadeh, R., Dehghani, M.H. and Yaghmaeian, K. (2021) Use of mine waste for H_2O_2-assisted heterogeneous Fenton-like degradation of tetracycline by natural pyrite nanoparticles: Catalyst characterization, degradation mechanism, operational parameters and cytotoxicity assessment. Journal of Cleaner Production 291, 125235.

Migaszewski, Z.M. and Gałuszka, A. (2019) The origin of pyrite mineralization: Implications for Late Cambrian geology of the Holy Cross Mountains (south-central Poland). Sedimentary Geology 390, 45-61.

Ministry of Natural Resources (2020) China Mineral Resources. http://www.mnr.gov.cn/sj/sjfw/kc_19263/zgkczybg/202010/P020201022261239245

1059.pdf.

Mohamed, U., Zhao, Y., Huang, Y., Cui, Y., Shi, L., Li, C., Pourkashanian, M., Wei, G., Yi, Q. and Nimmo, W. (2020) Sustainability evaluation of biomass direct gasification using chemical looping technology for power generation with and w/o CO_2 capture. Energy 205, 117904.

Morales-Gallardo, M.V., Ayala, A.M., Pal, M., Cortes Jacome, M.A., Toledo Antonio, J.A. and Mathews, N.R. (2016) Synthesis of pyrite FeS_2 nanorods by simple hydrothermal method and its photocatalytic activity. Chemical Physics Letters 660, 93-98.

Mousset, E., Huang Weiqi, V., Foong Yang Kai, B., Koh, J.S., Tng, J.W., Wang, Z. and Lefebvre, O. (2017) A new 3D-printed photoelectrocatalytic reactor combining the benefits of a transparent electrode and the Fenton reaction for advanced wastewater treatment. Journal of Materials Chemistry A 5(47), 24951-24964.

Mousset, E., Loh, W.H., Lim, W.S., Jarry, L., Wang, Z. and Lefebvre, O. (2021) Cost comparison of advanced oxidation processes for wastewater treatment using accumulated oxygen-equivalent criteria. Water Research 200, 117234.

Nichela, D.A., Donadelli, J.A., Caram, B.F., Haddou, M., Rodriguez Nieto, F.J., Oliveros, E. and García Einschlag, F.S. (2015) Iron cycling during the autocatalytic decomposition of benzoic acid derivatives by Fenton-like and photo-Fenton techniques. Applied Catalysis B: Environmental 170-171, 312-321.

Nidheesh, P.V. and Gandhimathi, R. (2012) Trends in electro-Fenton process for water and wastewater treatment: An overview. Desalination 299, 1-15.

Oh, W.D., Dong, Z. and Lim, T.T. (2016) Generation of sulfate radical through heterogeneous catalysis for organic contaminants removal: Current development, challenges and prospects. Applied Catalysis B: Environmental 194, 169-201.

Oliveira, M.L.S., Ward, C.R., Izquierdo, M., Sampaio, C.H., de Brum, I.A.S., Kautzmann, R.M., Sabedot, S., Querol, X. and Silva, L.F.O. (2012) Chemical composition and minerals in pyrite ash of an abandoned sulphuric acid production plant. Science of The Total Environment 430, 34-47.

Oral, O. and Kantar, C. (2019) Diclofenac removal by pyrite Fenton process: Performance in batch and fixed-bed continuous flow systems. Science of The Total Environment 664, 817-823.

Ouiriemmi, I., Karrab, A., Oturan, N., Pazos, M., Rozales, E., Gadri, A., Sanromán, M.Á., Ammar, S. and Oturan, M.A. (2017) Heterogeneous electro-Fenton using natural pyrite as solid catalyst for oxidative degradation of vanillic acid. Journal of Electroanalytical Chemistry 797, 69-77.

Peng, R., Yu, P. and Luo, Y. (2017) Coke plant wastewater posttreatment by Fenton and electro-Fenton processes. Environmental Engineering Science 34(2), 89-95.

Peng, S., Feng, Y., Liu, Y. and Wu, D. (2018) Applicability study on the degradation of acetaminophen via an H_2O_2/PDS-based advanced oxidation process using pyrite. Chemosphere 212, 438-446.

Qin, H., Jia, J., Lin, L., Ni, H., Wang, M. and Meng, L. (2018) Pyrite FeS_2 nanostructures: Synthesis, properties and applications. Materials Science and Engineering: B 236-237, 104-124.

Rahimi, F., van der Hoek, J.P., Royer, S., Javid, A., Mashayekh-Salehi, A. and Jafari Sani, M. (2021) Pyrite nanoparticles derived from mine waste as efficient catalyst for the activation of persulfates for degradation of tetracycline. Journal of Water Process Engineering 40, 101808.

Santos, C.S.C., Gabriel, B., Blanchy, M., Menes, O., García, D., Blanco, M., Arconada, N. and Neto, V. (2015) Industrial applications of nanoparticles – A prospective overview. Materials Today: Proceedings 2(1), 456-465.

Schellenbach, W.L. and Krekeler, M.P.S. (2012) Mineralogical and geochemical investigations of pyrite-rich mine waste from a kyanite mine in Central Virginia with comments on recycling. Environmental Earth Sciences 66(5), 1295-1307.

Setayesh, S.R., Nazari, P. and Maghbool, R. (2020) Engineered FeVO4/CeO2 nanocomposite as a two-way superior electro-Fenton catalyst for model and real wastewater treatment. Journal of Environmental Sciences 97, 110-119.

Shang, K., Li, W., Wang, X., Lu, N., Jiang, N., Li, J. and Wu, Y. (2019) Degradation of p-nitrophenol by DBD plasma/Fe^{2+}/persulfate oxidation process. Separation and Purification Technology 218, 106-112.

Si, Z., Song, X., Wang, Y., Cao, X., Wang, Y., Zhao, Y. and Ge, X. (2021) Natural pyrite improves nitrate removal in constructed wetlands and makes wetland a sink for phosphorus in cold climates. Journal of Cleaner Production 280, 124304.

Song, H., Yan, L., Wang, Y., Jiang, J., Ma, J., Li, C., Wang, G., Gu, J. and Liu, P. (2020) Electrochemically activated PMS and PDS: Radical oxidation versus nonradical oxidation. Chemical Engineering Journal 391, 123560.

Sun, L., Hu, D., Zhang, Z. and Deng, X. (2019) Oxidative degradation of methylene blue via PDS-based advanced oxidation process using natural pyrite. International Journal of Environmental Research and Public Health 16(23), 4773.

Tabelin, C.B., Igarashi, T., Villacorte-Tabelin, M., Park, I., Opiso, E.M., Ito, M. and Hiroyoshi, N. (2018) Arsenic, selenium, boron, lead, cadmium, copper, and zinc in naturally contaminated rocks: A review of their sources, modes of enrichment, mechanisms of release, and mitigation strategies. Science of The Total Environment 645, 1522-1553.

Trinh, T.K., Pham, V.T.H., Truong, N.T.N., Kim, C.D. and Park, C. (2017) Iron pyrite: Phase and shape control by facile hot injection method. Journal of Crystal Growth 461, 53-59.

Tsitonaki, A., Petri, B., Crimi, M., MosbÆk, H., Siegrist, R.L. and Bjerg, P.L. (2010) In situ chemical oxidation of contaminated soil and groundwater using persulfate: A review. Critical Reviews in Environmental Science and Technology 40(1), 55-91.

Vorontsov, A.V. (2019) Advancing Fenton and photo-Fenton water treatment through the catalyst design. Journal of Hazardous Materials 372, 103-112.

Wang, C., Sun, R., Huang, R. and Cao, Y. (2021) A novel strategy for enhancing heterogeneous Fenton degradation of dye wastewater using natural pyrite: Kinetics and mechanism. Chemosphere 272, 129883.

Wang, H., Chen, T., Chen, D., Zou, X., Li, M., Huang, F., Sun, F., Wang, C., Shu, D. and Liu, H. (2020a) Sulfurized oolitic hematite as a heterogeneous Fenton-like catalyst for tetracycline antibiotic degradation. Applied Catalysis B: Environmental

260, 118203.

Wang, J. and Wang, S. (2018) Activation of persulfate (PS) and peroxymonosulfate (PMS) and application for the degradation of emerging contaminants. Chemical Engineering Journal 334, 1502-1517.

Wang, X., Wang, Y., Chen, N., Shi, Y. and Zhang, L. (2020b) Pyrite enables persulfate activation for efficient atrazine degradation. Chemosphere 244, 125568.

Wu, D., Chen, Y., Zhang, Y., Feng, Y. and Shih, K. (2015) Ferric iron enhanced chloramphenicol oxidation in pyrite (FeS_2) induced Fenton-like reactions. Separation and Purification Technology 154, 60-67.

Wu, D., Chen, Y., Zhang, Z., Feng, Y., Liu, Y., Fan, L. and Zhang, Y. (2016a) Enhanced oxidation of chloramphenicol by GLDA-driven pyrite induced heterogeneous Fenton-like reactions at alkaline condition. Chemical Engineering Journal 294, 49-57.

Wu, D., Feng, Y. and Ma, L. (2013) Oxidation of azo dyes by H_2O_2 in presence of natural pyrite. Water, Air, & Soil Pollution 224(2), 1407.

Wu, D., Liu, Y., He, H. and Zhang, Y. (2016b) Magnetic pyrite cinder as an efficient heterogeneous ozonation catalyst and synergetic effect of deposited Ce. Chemosphere 155, 127-134.

Wu, L., Lin, Q., Fu, H., Luo, H., Zhong, Q., Li, J. and Chen, Y. (2022) Role of sulfide-modified nanoscale zero-valent iron on carbon nanotubes in nonradical activation of peroxydisulfate. Journal of Hazardous Materials 422, 126949.

Xiao, S., Cheng, M., Zhong, H., Liu, Z., Liu, Y., Yang, X. and Liang, Q. (2020) Iron-

mediated activation of persulfate and peroxymonosulfate in both homogeneous and heterogeneous ways: A review. Chemical Engineering Journal 384, 123265.

Yu, F., Wang, Y., Ma, H. and Zhou, M. (2020) Hydrothermal synthesis of FeS_2 as a highly efficient heterogeneous electro-Fenton catalyst to degrade diclofenac via molecular oxygen effects for Fe(II)/Fe(III) cycle. Separation and Purification Technology 248, 117022.

Zeng, L., Gong, J., Dan, J., Li, S., Zhang, J., Pu, W. and Yang, C. (2019) Novel visible light enhanced Pyrite-Fenton system toward ultrarapid oxidation of p-nitrophenol: Catalytic activity, characterization and mechanism. Chemosphere 228, 232-240.

Zhan, Y., Yan, N., Fei, G., Xia, H. and Meng, Y. (2020) Crack growth resistance of natural rubber reinforced with carbon nanotubes. Journal of Applied Polymer Science 137(10), 48447.

Zhang, H., Wang, Z., Liu, C., Guo, Y., Shan, N., Meng, C. and Sun, L. (2014a) Removal of COD from landfill leachate by an electro/Fe^{2+}/peroxydisulfate process. Chemical Engineering Journal 250, 76-82.

Zhang, M., Dong, H., Zhao, L., Wang, D. and Meng, D. (2019a) A review on Fenton process for organic wastewater treatment based on optimization perspective. Science of The Total Environment 670, 110-121.

Zhang, N., Chen, J., Fang, Z. and Tsang, E.P. (2019b) Ceria accelerated nanoscale zerovalent iron assisted heterogenous Fenton oxidation of tetracycline. Chemical Engineering Journal 369, 588-599.

Zhang, N., Xian, G., Li, X., Zhang, P., Zhang, G. and Zhu, J. (2018a) Iron Based

Catalysts Used in Water Treatment Assisted by Ultrasound: A Mini Review. Frontiers in Chemistry 6(12).

Zhang, P., Huang, W., Ji, Z., Zhou, C. and Yuan, S. (2018b) Mechanisms of hydroxyl radicals production from pyrite oxidation by hydrogen peroxide: Surface versus aqueous reactions. Geochimica et Cosmochimica Acta 238, 394-410.

Zhang, Y., Tran, H.P., Du, X., Hussain, I., Huang, S., Zhou, S. and Wen, W. (2017) Efficient pyrite activating persulfate process for degradation of p-chloroaniline in aqueous systems: A mechanistic study. Chemical Engineering Journal 308, 1112-1119.

Zhang, Y., Zhang, K., Dai, C., Zhou, X. and Si, H. (2014b) An enhanced Fenton reaction catalyzed by natural heterogeneous pyrite for nitrobenzene degradation in an aqueous solution. Chemical Engineering Journal 244, 438-445.

Zhao, Q., Mao, Q., Zhou, Y., Wei, J., Liu, X., Yang, J., Luo, L., Zhang, J., Chen, H., Chen, H. and Tang, L. (2017) Metal-free carbon materials-catalyzed sulfate radical-based advanced oxidation processes: A review on heterogeneous catalysts and applications. Chemosphere 189, 224-238.

Zhou, Y., Huang, M., Wang, X., Gao, J., Fang, G. and Zhou, D. (2020) Efficient transformation of diethyl phthalate using calcium peroxide activated by pyrite. Chemosphere 253, 126662.

Zhou, Y., Wang, X., Zhu, C., Dionysiou, D.D., Zhao, G., Fang, G. and Zhou, D. (2018) New insight into the mechanism of peroxymonosulfate activation by sulfur-containing minerals: Role of sulfur conversion in sulfate radical generation. Water

Research 142, 208-216.

Zhu, X., Li, J., Xie, B., Feng, D. and Li, Y. (2020) Accelerating effects of biochar for pyrite-catalyzed Fenton-like oxidation of herbicide 2,4-D. Chemical Engineering Journal 391, 123605.

Figure 1

Fig. 1. Typical processes of pretreating natural pyrite and preparing synthetic pyrite for the applications in AOPs.

Figure 2

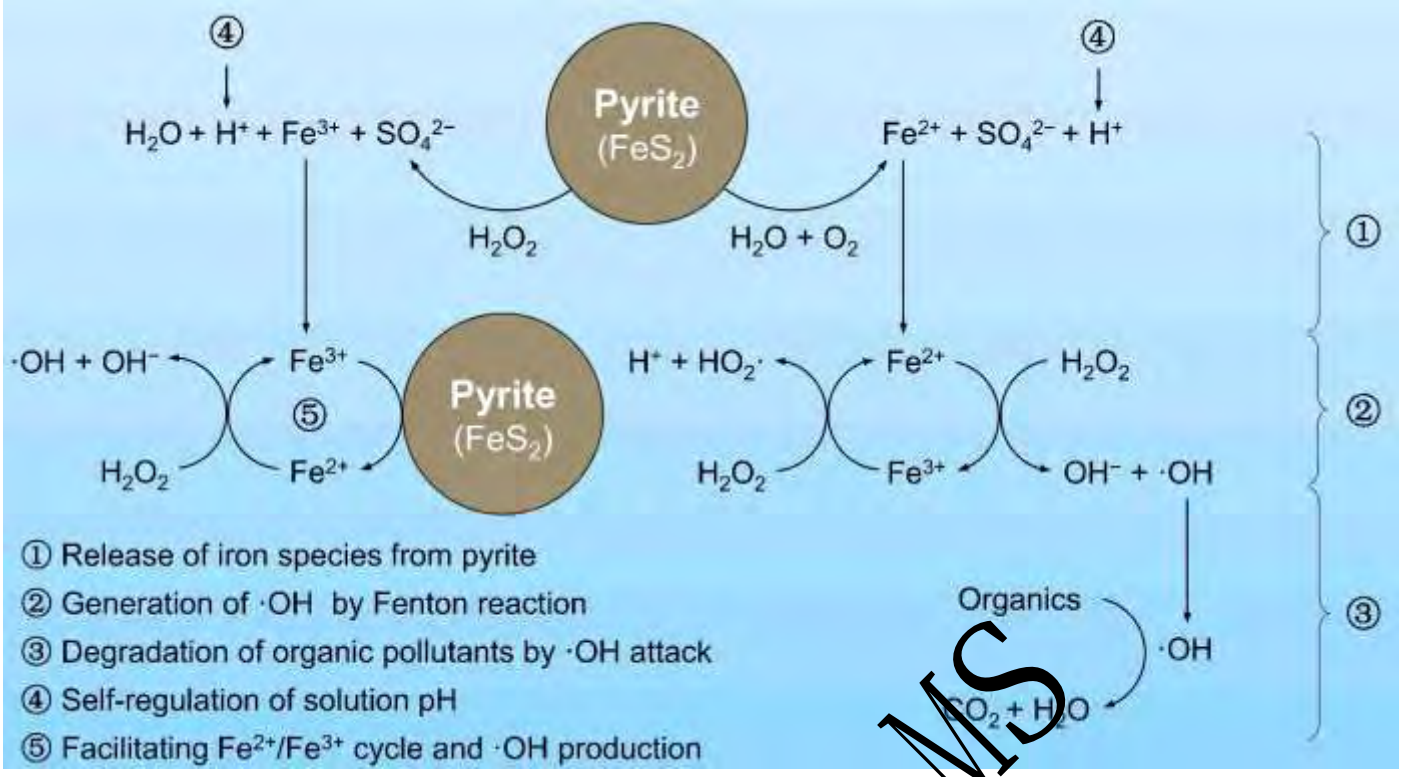

Fig. 2. Proposed mechanisms of pyrite-mediated Fenton oxidation processes for the degradation of organic pollutants.

Figure 3

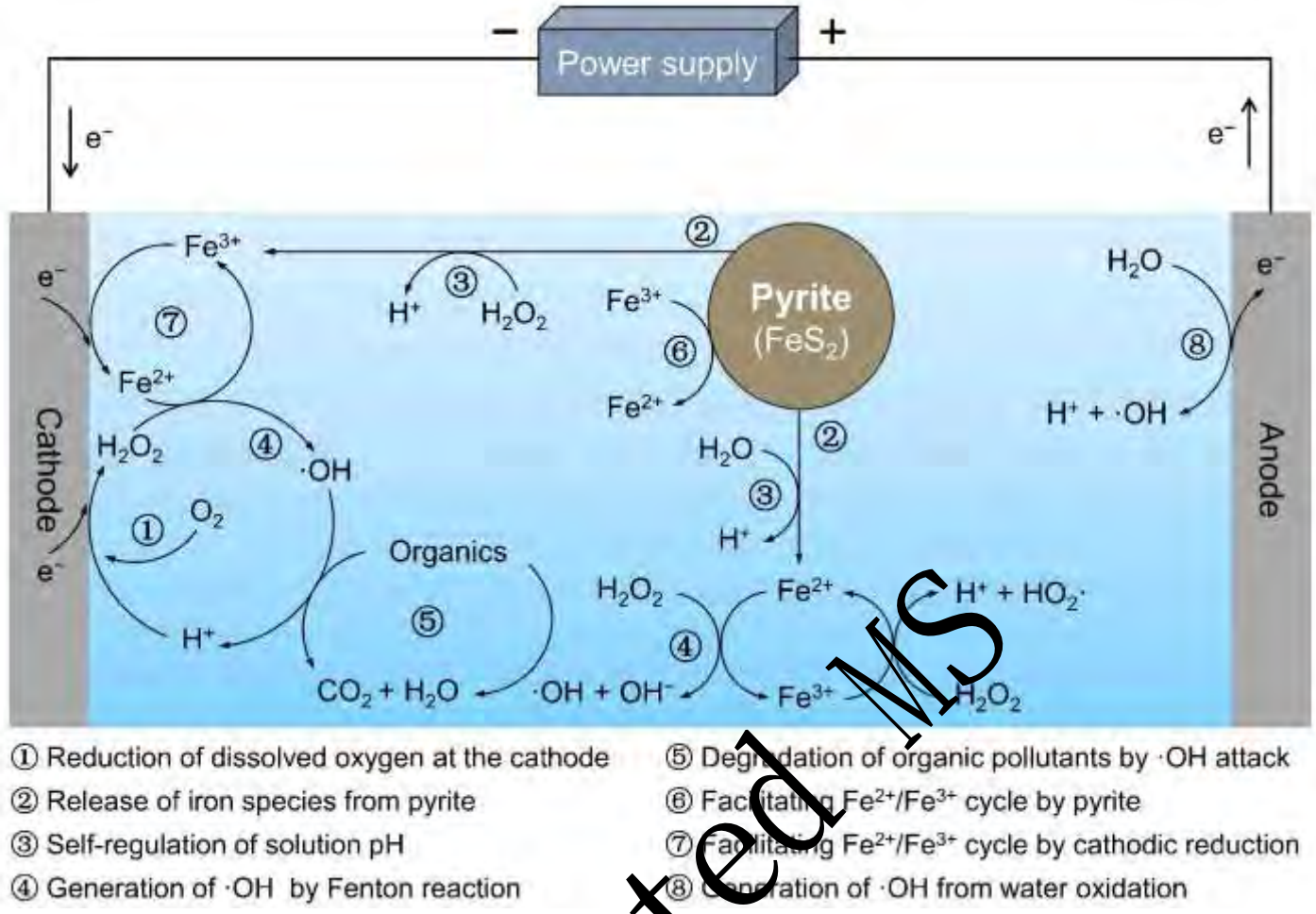

Fig. 3. Proposed mechanisms of pyrite-mediated electro-Fenton oxidation processes for the degradation of organic pollutants.

Figure 4

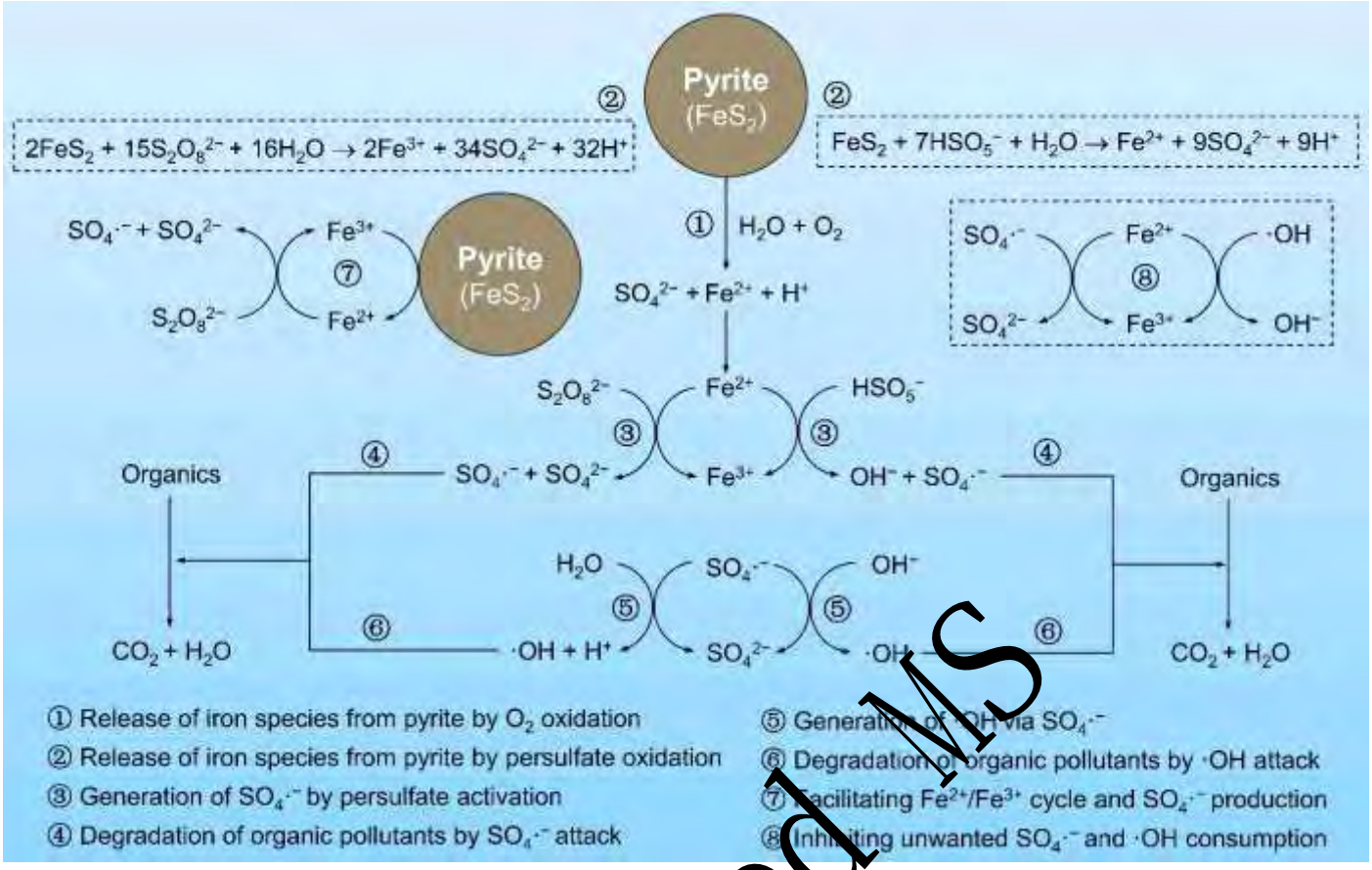

Fig. 4. Proposed mechanisms of pyrite-mediated persulfate oxidation processes for the degradation of organic pollutants.

Figure 5

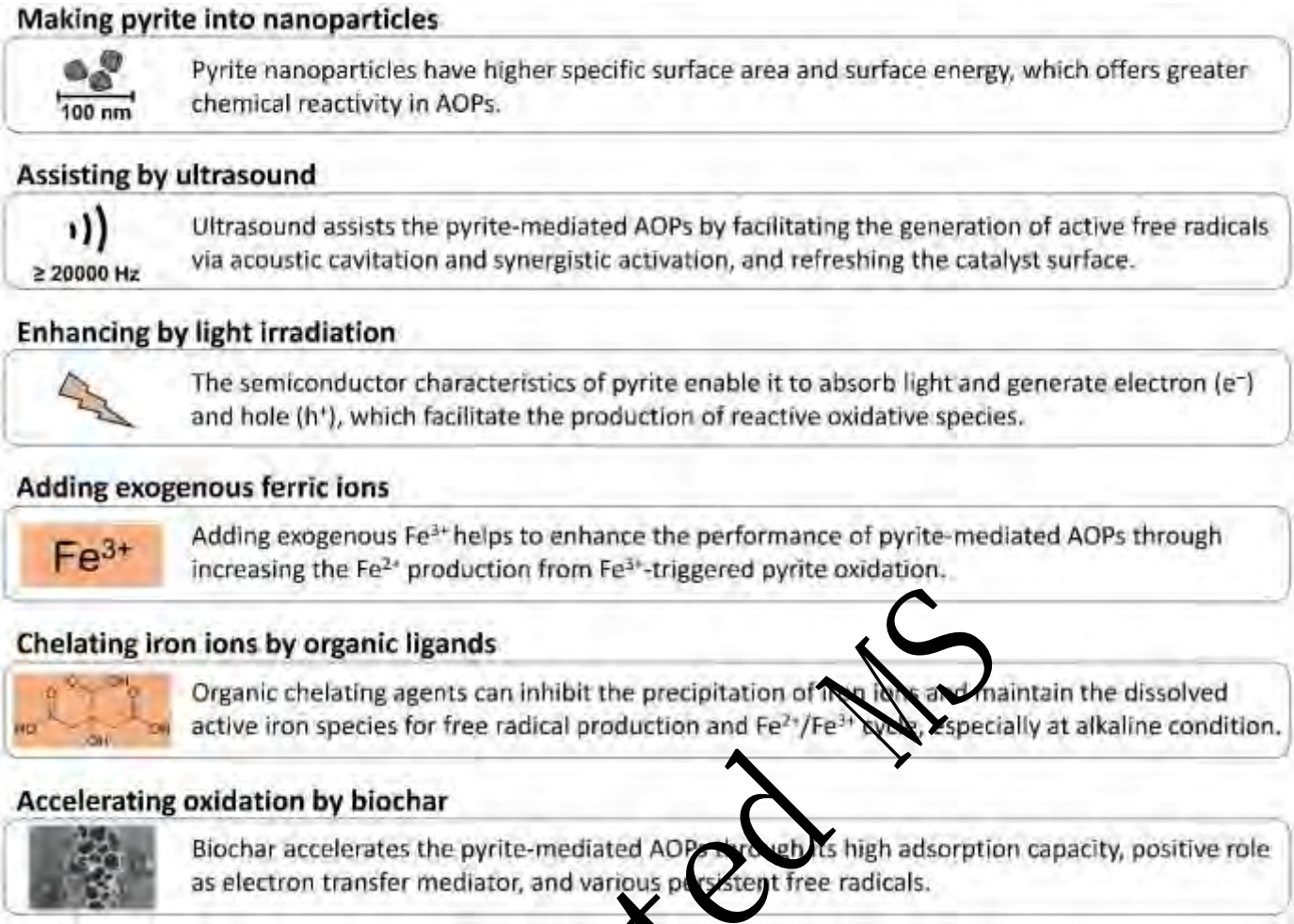

Fig. 5. Some strategies to enhance the performance of pyrite-mediated AOPs for the degradation of organic pollutants.

Figure 6

Fig. 6. Main advantages of pyrite as a catalyst for AOPs.

Table 1 Applications of pyrite in Fenton oxidation processes.

Targeted pollutant	Optimal reaction conditions	Performance	Highlighted conclusion	Reference
Methylene blue (MB)	Pyrite dosage: 0.83 g/L[a] H_2O_2 concentration: 33 mmol/L[a] pH: 6.2 C_0[b]: 10 mg/L	The MB was effectively degraded within 20 min.	The self-regulation of pH and Fe^{2+}/Fe^{3+} cycle promote the ·OH production and thus the MB degradation.	Wang et al. (2021)
Tetracycline	Pyrite dosage: 1.0 g/L H_2O_2 concentration: 5.0 mmol/L pH: 4.1 C_0: 50 mg/L	The tetracycline was completely degraded within 60 min, with a mineralization efficiency over 85%.	The main reactive oxygen species is ·OH, which is produced by the interactions between H_2O_2 and pyrite surface, and between the surface sulfur-defects and H_2O.	Mashayekh-Salehi et al. (2021)
Diclofenac	Pyrite dosage: 1.0 g/L H_2O_2 concentration: 0.3 mol/L pH: 5.1 C_0: 100 mg/L	About 60% of the TOC was removed within 10 min.	The ·OH generation depends on the rate of Fe dissolution from pyrite.	Oral and Kantar (2019)
Chlorophenols	Pyrite dosage: 1.0 g/L H_2O_2 concentration: 0.3 mol/L pH: 3.0 C_0: 100 mg/L	All the chlorophenols was completely degraded within 40 min, but a significant portion of the TOC still remained.	The removal of polychlorinated phenol is driven by ·OH attack and sorption onto pyrite.	Kantar et al. (2019b)
Acetaminophen	Pyrite dosage: 2.0 g/L H_2O_2 concentration: 5.0 mmol/L pH: 4.0 C_0: 50 mg/L	Within 180 min, 96.6% of the acetaminophen was degraded.	Under alkaline conditions, the formation of Fe(III)-O on pyrite surface lowers the ·OH generation.	Peng et al. (2018)
Rhodamine B	Pyrite dosage: 1.0 g/L H_2O_2 concentration: 6.0 mmol/L pH: 3.0 C_0: 19.16 mg/L	Within 120 min, 99% of the Rhodamine B was degraded.	The reaction between the dissolved Fe^{2+} from pyrite and H_2O_2 are the main activation mechanism for Rhodamine B degradation.	Diao et al. (2017)
Alachlor	Pyrite dosage: 0.5 g/L H_2O_2 concentration: 0.8 mmol/L pH: 6.2 C_0: 0.074 mmol/L	Over 99% of the alachlor was degraded within 60 min.	The O_2 activation by more surface-bound Fe^{2+} on pyrite generates $\cdot O_2^-$, which facilitates the Fe^{2+}/Fe^{3+} cycle and the ·OH production.	Liu et al. (2015)
Nitrobenzene	Pyrite dosage: 2.0 g/L H_2O_2 concentration: 0.25 mol/L pH: 3.0 C_0: 20 mg/L	Within 300 min, 80% of the nitrobenzene was degraded.	The Fe^{2+} concentration in pyrite/H_2O_2 system is low but adequate for the catalytic degradation of nitrobenzene.	Zhang et al. (2014b)
Reactive black 5 and acid red GR	Pyrite dosage: 0.3 g/L H_2O_2 concentration: 0.3 mmol/L pH: 6.96 (for reactive black 5) and 6.32 (for acid red GR) C_0: 50 mg/L	Within 10 min, 85% of the reactive black 5 and the acid red GR was removed.	The $FeSO_4$ formed on pyrite surface releases high level of Fe^{2+} for initiating Fenton reaction.	Wu et al. (2013)

[a] In order to show the results in a unified form, the data was obtained by recalculation according to the reference.

[b] C_0 represents the initial pollutant concentration.

Table 2 Applications of pyrite in electro-Fenton oxidation processes.

Targeted pollutant	Optimal reaction conditions	Performance	Highlighted conclusion	Reference
Diclofenac	Pyrite dosage: 8.0 g/L[a] Current density: 100 mA[a] pH: 7.0 C_0[b]: 50 mg/L	Within 180 min, 85% of the TOC was removed.	The molecular O_2 activation by more surface-bound Fe^{2+} on pyrite generates $\cdot O_2^-$, which facilitates the Fe^{2+}/Fe^{3+} cycle.	Yu et al. (2020)
Vanillic acid	Pyrite dosage: 1.0 g/L Current: 300 mA pH: 3.0 C_0: 0.1 mmol/L	Within 240 min, 89.2% of the TOC was removed.	Pyrite can be used as a solid catalyst to provide Fe^{2+} for electro-Fenton process.	Ouiriemmi et al. (2017)
Tetracycline	Pyrite dosage: 2.0 g/L Current: 300 mA pH: 3.0 C_0: 0.2 mmol/L	Within 480 min, 96% of the TOC was removed.	Pyrite supports the self-regulation of soluble Fe^{2+} and pH.	Barhoumi et al. (2017)
Sulfamethazine	Pyrite dosage: 2.0 g/L Current: 300 mA pH: 3.0 C_0: 0.2 mmol/L	Within 480 min, 95% of the TOC was removed.	The boron doped diamond electrode shows greater performance than Pt electrode in pyrite-electro-Fenton system.	Barhoumi et al. (2016)
4-amino-3-hydroxy-2-*p*-tolylazo-naphthalene-1-sulfonic acid (AHPS)	Pyrite dosage: 2.0 g/L Current: 300 mA pH: 3.0 C_0: 175 mg/L	Almost complete removal of the TOC was achieved within 480 min.	Pyrite mediated electro-Fenton process is more cost effective than classical one.	Labiadh et al. (2015)
Levofloxacin	Pyrite dosage: 1.0 g/L Current: 300 mA pH: 3.0 C_0: 0.23 mmol/L	Within 480 min, 95% of the TOC was removed.	Pyrite provides soluble Fe^{2+} and regulates the solution pH.	Barhoumi et al. (2015)
Tyrosol	Pyrite dosage: 1.0 g/L Current: 300 mA pH: 3.0 C_0: 0.3 mmol/L	Within 360 min, 89% of the TOC was removed.	Pyrite spontaneously regulates the pH to an optimal value of 3.0.	Ammar et al. (2015)

[a] In order to show the results in a unified form, the data was obtained by recalculation according to the reference.

[b] C_0 represents the initial pollutant concentration.

Table 3 Applications of pyrite in persulfate oxidation processes.

Targeted pollutant	Optimal reaction conditions	Performance	Highlighted conclusion	Reference
Propanil	Pyrite dosage: 0.5 g/L PMS concentration: 1.0 mmol/L pH: 2.9 C_0: 0.01 mmol/L	Within 15 min, 91.9% of the propanil was degraded.	In the pyrite/PMS system, $SO_4{\cdot}^-$ and ·OH are the dominant reactive species.	Li et al. (2021)
Tetracycline	Pyrite dosage: 1.0 g/L PDS/PMS concentration: 1.0 g/L pH: 4.1 C_0: 50 mg/L	Within 30 min, the removal rate of tetracycline in PDS and PMS system was 32.5% and 98.7%, respectively.	Both ·OH and $SO_4{\cdot}^-$ are generated in pyrite/PMS system, and $SO_4{\cdot}^-$ is more dominant.	Rahimi et al. (2021)
2,4-dichlorophenol	Pyrite dosage: 1.0 g/L PDS concentration: 1.0 mmol/L pH: 5.0 C_0: 30 mg/L	Within 120 min, 81.2% of the 2,4-DCP was degraded.	The reductive low-valence sulfur on pyrite plays a key role in the Fe^{2+}/Fe^{3+} cycle.	He et al. (2021)
Atrazine	Pyrite dosage: 4.2 mmol/L PDS concentration: 3.0 mmol/L pH: 7.0 C_0: 20 mg/L	Atrazine was completely degraded within 45 min, with 26% of the TOC removal within 420 min.	The slow and sustainable Fe^{2+} release from pyrite inhibits the quenching reaction between $SO_4{\cdot}^-$/·OH and Fe^{2+}.	Wang et al. (2020b)
Acid orange 7	Pyrite dosage: 4.0 g/L PDS concentration: 0.4 g/L pH: 2.5–2.7 C_0: 20 mg/L	Within 30 min, 99% of the acid orange 7 was degraded.	The major reactive oxygen species in pyrite/PDS system are $SO_4{\cdot}^-$, O_2^-, and $^1O_2$.	Li et al. (2020b)
Nonylphenol	Pyrite dosage: 0.85 g/L PDS concentration: 5.85 mmol/L pH: 3.0 C_0: 10 μmol/L	Over 99% of the nonylphenol was degraded and 80% of the TOC was removed within 90 min.	The coexisting ions inhibits the nonylphenol degradation in the following order: $PO_4^{3-} > HCO_3^- > Cu^{2+} > NO_3^- > Ca^{2+} > NH_4^+$.	Asgari et al. (2020)
Methylene blue	Pyrite dosage: 0.5 g/L PDS concentration: 2.0 mmol/L pH: 5.0 C_0: 100 mg/L	Almost complete removal of the methylene blue was achieved within 120 min.	The strong acid-production ability of pyrite/PDS system prevents the passivation of pyrite surface.	Sun et al. (2019)
Acetaminophen	Pyrite dosage: 2.0 g/L PDS concentration: 5.0 mmol/L pH: 4.0 C_0: 50 mg/L	The acetaminophen was completely degraded within 180 min.	High acid-yield favors the pyrite surface exposure in pyrite/PDS system.	Peng et al. (2018)
1,4-dioxane	Pyrite dosage: 5.0 g/L PMS/PDS concentration: 2.3	In pyrite/PMS system, almost complete removal of the 1,4-dioxane was	The disulfide in pyrite plays a significant role in the Fe^{2+} release.	Feng et al. (2018)

	mmol/L pH: 7.0 C_0: 50 mg/L	achieved within 40 min.		
Ethylthionocarbamate	Pyrite dosage: 1.0 g/L PDS concentration: 0.12 g/L pH: 3.0 C_0: 30 mg/L	Within 180 min, 96.64% of the ethylthionocarbamate was degraded.	The predominant reactive species is $SO_4^{\cdot -}$ in pyrite/PDS system.	Chen et al. (2018)
p-chloroaniline	Pyrite dosage: 0.5 g/L PDS concentration: 0.5 mmol/L pH: 7.0 C_0: 0.1 mmol/L	Almost complete removal of the *p*-chloroaniline was achieved within 60 min.	The generated $\cdot O_2$ enhances the activation of PDS to produce more $SO_4^{\cdot -}$.	Zhang et al. (2017)
Methyl *tert*-butyl ether	Pyrite dosage: 3.0 g/L PDS concentration: 5.0 g/L pH: ~5.5 C_0: 60 mg/L	Complete degradation of the methyl *tert*-butyl ether can be achieved within 240 min.	The predominant reactive species is $SO_4^{\cdot -}$ in pyrite/PDS system.	Liang et al. (2010)

Table 4 Comparison of pyrite-mediated AOP systems with other AOP systems.

AOP systems	Targeted pollutant	Difficulty Level of catalyst preparation[a]	Treatment efficiency	Material cost	Reference
Pyrite-mediated Fenton oxidation	Tetracycline	+ (natural pyrite)	The tetracycline was completely degraded within 60 min, with a mineralization efficiency over 85%.	\$100–300/t[b]	Mashayekh-Salehi et al. (2021)
Pyrite-mediated electro-Fenton oxidation	Tetracycline	+ (natural pyrite)	Within 480 min, 96% of the TOC was removed.	\$100–300/t	Barhoumi et al. (2017)
Pyrite-mediated persulfate oxidation	Tetracycline	+ (natural pyrite)	Within 30 min, the removal rate of tetracycline in PDS and PMS system was 32.5% and 98.7%, respectively.	\$100–300/t	Rahimi et al. (2021)
Fe^0/CeO_2-mediated Fenton oxidation	Tetracycline	+++ (precipitation and $NaBH_4$ reduction method)	Within 60 min, about 90% of the tetracycline was degraded.	\$15/g[c]	Zhang et al. (2019)
Sulfurized oolitic hematite- mediated Fenton oxidation	Tetracycline	++ (annealing oolitic hematite in hydrogen sulfide)	Within 60 min, about 90% of the tetracycline was degraded.	\$95/ton[d]	Wang et al. (2020a)
$FeVO_4/CeO_2$-mediated electro-Fenton oxidation	Methyl orange	++ (hydrothermal method)	Within 60 min, 96.31% of the methyl orange and 70% of the chemical oxygen demand were removed.	About \$1000/ton[e]	Setayesh et al. (2020)
S-nZVI@CNTs-mediated persulfate oxidation	Sulfamethoxazole	+++ (purification and liquid-phase reduction method)	Within 40 min, complete degradation of sulfamethoxazole was achieved.	\$15/g (nZVI) and \$100/kg (CNTs)[f]	Wu et al. (2022)
$ZrO_2/MnFe_2O_4$-mediated persulfate oxidation	Tetracycline	++ (low-temperature co-precipitation method)	Within 120 min, 85.2% of the tetracycline was degraded.	\$10/kg[g]	Liu et al. (2021)

[a] Difficult: +++; medium: ++; easy: +.
[b] The material cost of natural pyrite is displayed as its current market price (Hu et al. 2020).
[c] This is just the market price of nano-Fe^0 according to the report by Gao et al. (2021).
[d] This is the price of hematite according to the report by Mohamed et al. (2020).
[e] This is just the price of CeO_2 according to the report by Herget et al. (2017).
[f] The price of carbon nanotubes (CNTs) is given in the report by Zhan et al. (2020).
[g] This is just the price of ZrO_2 according to the report by Bagnato et al. (2019).